KURENAI
Kyoto University Research Information Repository

KYOTO UNIVERSITY

Title	BAND-TYPE DISSIPATIVE STRUCTURES IN BIOLOGICAL SYSTEMS(Theory of Dynamical Systems and Its Application to Nonlinear Problems)
Author(s)	TOKO, Kiyoshi; YAMAFUJI, Kaoru
Citation	(1984), 536: 249-265
Issue Date	1984-09
URL	http://hdl.handle.net/2433/98669
Right	
Type	Departmental Bulletin Paper
Textversion	publisher

Kyoto University

BAND-TYPE DISSIPATIVE STRUCTURES IN BIOLOGICAL SYSTEMS

Kiyoshi TOKO and Kaoru YAMAFUJI

都甲 潔 , 山藤 馨

Department of Electronics
Faculty of Engineering
Kyushu University 36
Fukuoka 812, Japan

Band-type electric patterns in many-cell as well as
unit-cell biological systems are investigated. Growing
roots of azuki bean are found to display bands of surface
electric potential in a mature region when they reach
ten cm or so. Together with an experimental result of
electric isolation, the electric current is supposed to
flow into an elongation zone while accompanied by local
current loops in the mature region. To clarify a formation
mechanism of bands observed in the Characean algae and
bean roots, a simplified model system is treated numeri-
cally and analytically. The results reveal that the
band pattern is a dissipative structure appearing far
from equilibrium.

1. Introduction

A spatial pattern of electric current has been observed in many
biological systems.[1-5] It appears most evidently in growing or regene-
rating cells. For example, a rhizoid formation in the brown alga *Fucus*
is accompanied by an electric current pattern around and within the
egg.[1] A causal relationship between the electric current and the spa-
tial distribution of molecules inside and on the surface of egg is
expected for an appearance of polarity after fertilization. In fact,
a theory[6] based on nonequilibrium thermodynamics has shown that the
rhizoid formation is one of the typical self-organization processes
appearing in far-from-equilibrium conditions. It occurs through a
nonlinear coupling between ion flux and the accumulation of membrane-
constituting molecules. These macroscopic electric patterns can
therefore be regarded as dissipative structures realizing far from
equilibrium.[7]

The present study is concerned with a band-type electric pattern
in biological systems. As one example of electric patterns in growing

many-cell systems, we measured an electric potential near the surface
of roots of azuki bean. A band-type pattern of potential was revealed
while the potential declines as a whole from the root base to the root
tip. Another example provided here is related to a well-known band-type
pattern of electric potential or pH near the surface of internodal or
whorl cell of the Characean algae.[4] A theoretical analysis shows
that this pattern corresponds to a dissipative structure. These kinds
of bands in biological systems can be understood as essentially the same
as the band pattern in B-Z reaction[7] or the Liesegang ring.[8]

2. Band-Type Pattern in Bean Roots

2.1 Materials and method

Seeds of azuki bean (*Phaseolus chrysanthos*) were soaked for three
hours and then were sown on filter papers moistened with 0.01mM KCl in
darkness at about 30°C. Figure 1 shows the experimental setup for
measurements of the electric potential near the root surface.

The growth speed at each point of root was studied by making india
ink dots at 1mm intervals along the root surface. Five hours later the
change in each interval was measured. The relative growth (RG) is
calculated, with $\tilde{e}$ the elongation of each district and E the total
elongation, by

$$RG = (\tilde{e}/E) \times 100 \quad (\%) . \qquad (1)$$

The pH near the root was measured using pH meter (CORNING, model
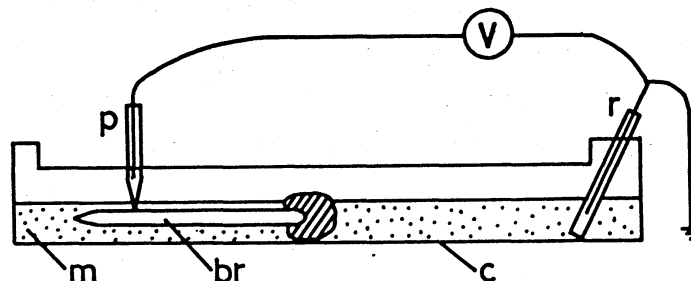125) equipped with pH electrode (IWAKI GLASS, model IW202). The tip

Fig.1 Schematic illustration of experimental
setup. p, pippete electrode; r, reference
electrode; br, bean root; c, chamber; m, 0.01
mM KCl medium.

diameter of the electrode is smaller than 1mm.

2.2 Experimental results

Figure 2 shows an example of observed surface potential for a 13.3 cm length root.[9] A periodic spatial change in potential with the period of about 2cm can be seen. This kind of pattern usually appeared when the root reached ten cm length or so. So far as the root was short, the surface potential had only one convex peak around the position of (5-20)mm behind the root tip and the successive concave peak around (20-35)mm, as is well known.[3] The result in Fig.2 also demonstrates that the surface potential near the root base is more positive than the potential near the root tip on the whole. As shown in Fig.3, the spatial potential pattern forms a band structure surrounding the root.[9]

The band-type potential pattern was fairly stable in each root: The similar patterns were obtained when the measurements were repeated within such a short interval as one hour or less. However, roots grew with remarkable elongation velocity of about 1.5mm/hr and hence, in the long run the potential changed slowly accompanied by the elongation.
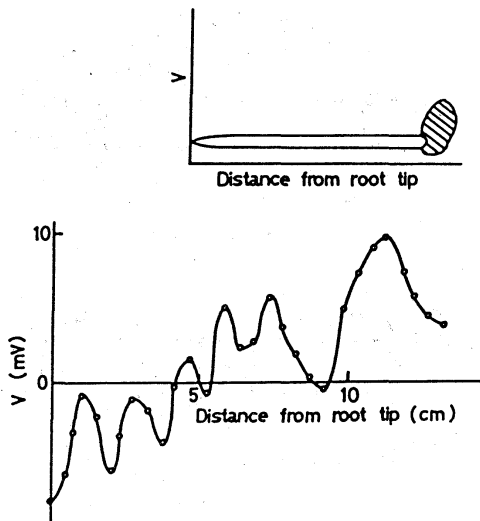

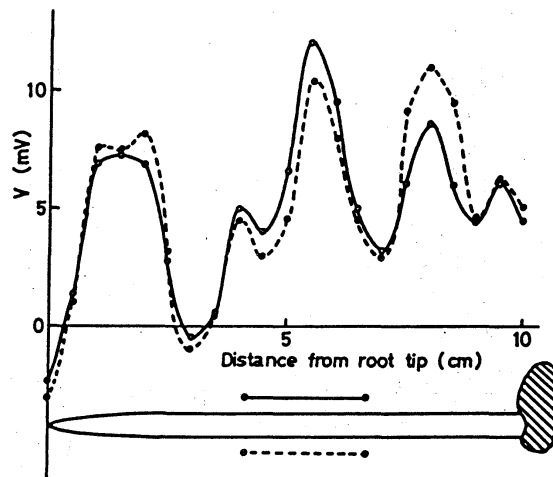Fig.2 Pattern of surface electric potential V when the root grows up to 13.3 cm length.

Fig.3 Symmetry of potential pattern on the opposite sides of root surface.

This led to the production of another band with the splitting of one band to two bands. In this way, longer roots showed more bands.

Figure 4 shows a relationship between the relative growth and the surface electric potential:[9] The elongation zone was located at 1 to 2mm behind from the tip, whereas the surface potential has a peak around 7mm behind. This means that the elongation zone lies in the relatively negative region of surface potential. Thus, it suggests the electric current flowing out of the potential-peak position into the elongation zone. To confirm this anticipation, we made an electric isolation of the elongation zone from the mature region. The experiment showed that the electric isolation effectively represses the growth of root so as to reduce the usual growth rate, 1.5mm/hr, to 0.5mm/hr.

Next, we must know what kind of ion species participates in the growth. Taking into account an acid-growth mechanism,[10] we measured
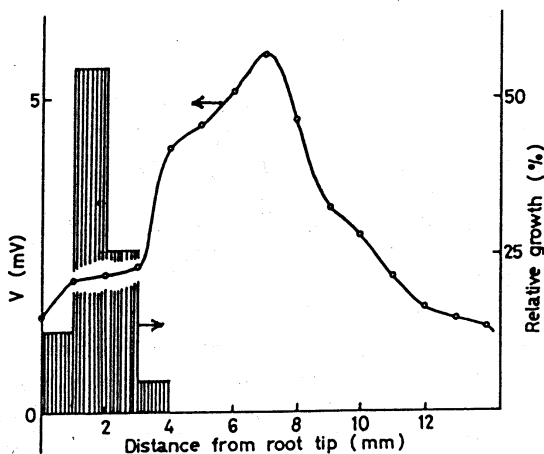

Fig.4 Relative growth and surface potential pattern. Note the scale in the mm unit.
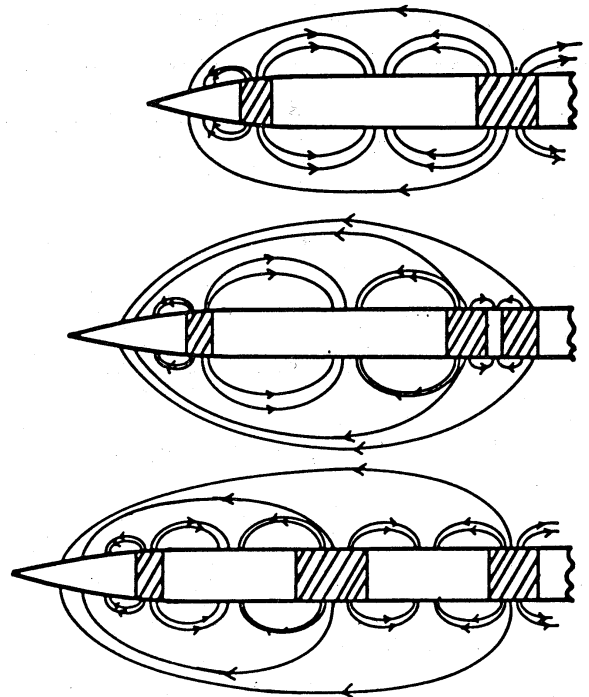
Fig.5 Schematic illustration of a relationship between the electric current pattern and the growth.

the pH near the surface in elongation and mature regions. Table 1 summarizes the result. The decrease in pH of the measuring point from the external bulk solution (pH 6.8) is shown. This result implies that

Table 1. Change in pH near the root

	elongation zone	mature region
Control	0.53	0.46
Electric isolation	0.31	0.80

the growth rate diminishes due to the suppression of acidification in the elongation zone in the case of electric isolation, while roots continue to grow mediated by the acidification in usual conditions. Protons can therefore be considered to flow out from the mature region and flow into the elongation zone.

As a consequence, we can image the causal relationship between the electric current pattern and the growth. Figure 5 illustrates the electric current flowing into the elongation zone accompanied by local current loops in the mature region. The elongation zone can grow with the supply of H^+ mediated by electric current produced in the mature region.

3. Dissipative Structure in the *Characeae*

The Characean algae as *Nitella* and *Chara* develop alternating acid and alkaline bands along their cell walls under illumination.[4,11] An electric potential near the cell surface also shows a similar band-type pattern, and hence an electric current flows from the acid to the alkaline zones. It is supposed that the acid zones are produced by an active H^+ efflux or equivalent OH^- influx. In the present section, we try to demonstrate the band structure as a dissipative structure appearing far from equilibrium.[12]

3.1 A theoretical model

Figure 6 shows the model system, where a Characean internodal cell with the radius R lies between z=0 and L surrounded by the external aqueous solution. Since the band pattern can appear prior to any
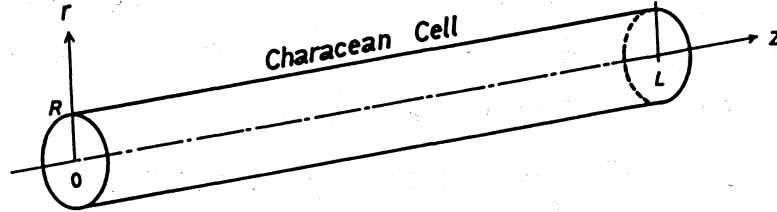
<u>Fig.6</u> A theoretical model system.

pattern with circumferential symmetry breaking,[13] the angular depend-
ence is not taken into account here.

Let us denote the H^+ concentration by $n(r,z,t)$ with t the time,
then a diffusion equation for n in the external environment and the
cytoplasm is given by

$$\frac{\partial n}{\partial t} = D\left[\frac{1}{r}\frac{\partial}{\partial r}\left(r\frac{\partial}{\partial r}\right) + \frac{\partial^2}{\partial z^2}\right] n \ , \tag{2}$$

where D is the diffusion constant, values of which in the cell exterior
and interior are taken as equal.

Let us next introduce simplified expressions for a passive flux,
J_p, and an active flux, J_a, produced by H^+-ATPase molecules within the
membrane at r=R. We adopt the linear relation for J_p:

$$J_p = -p \, \Delta n \ , \tag{3}$$

where p denotes the permeability, and the H^+-concentration difference
Δn is defined by

$$\Delta n(z,t) = n_{es}(z,t) - n_{is}(z,t) \ . \tag{4}$$

The values of H^+ concentration at the external (r=R+0) and internal
(r=R-0) surfaces of plasmalemma are respectively designated by n_{es}
and n_{is}. The efflux is taken as plus sign.

As for the active flux J_a, we assume the following nonlinear
function of internal variables h and Δn:

$$J_a = \frac{\alpha}{1 + \exp[(h-\Delta n)/\gamma]} \ , \tag{5}$$

with α denoting the maximum active-flux density of protons when all H^+-ATPase are activated. The coefficient $1/\gamma$ represents a sharpness of the sigmoid curve as an increasing function of Δn. The internal variable h expresses an inhibitory factor for the pump activation.

Light may produce ATP as an energy source of H^+ pumps via complex chemical reactions with many steps. In the present stage, it is natural to assume the following simple relation for the light intensity I:

$$J_a^T = a I , \tag{6}$$

where a is the numerical coefficient, and the average active flux J_a^T is defined by

$$J_a^T = \frac{1}{L} \int_0^L J_a \, dz . \tag{7}$$

The boundary condition on the Characean cell membrane at r=R is expressed by the flux continuity across the membrane as

$$-D\left(\frac{\partial n_e}{\partial r}\right)_s = -D\left(\frac{\partial n_i}{\partial r}\right)_s = J_p + J_a \qquad \text{at } r=R . \tag{8}$$

The boundary conditions inside the cell ($0 \le r < R$, $0 \le z \le L$) are the nonflux ones:

$$\partial n/\partial z = 0 \qquad \text{at } z=0 \ \& \ L, \quad 0 \le r < R ,$$

$$\partial n/\partial r = 0 \qquad \text{at } r=0 , \quad 0 \le z \le L . \tag{9}$$

In the external solution a selection of the boundary condition scarcely alters the obtained results, and hence explicit equations are not shown here (see details[12]).

The present model system has the following characteristics:

i) The kinetic equation (2) holding in the cell interior and exterior is a linear function.

ii) The boundary condition (8) with eqs.(3) and (5) is nonlinear and time-dependent.

iii) The average active flux J_a^T is restricted by the light intensity I in eqs.(6) and (7).

3.2 Numerical results

Figures 7(a) and (b) express a homogeneous flux pattern and a band pattern with a single acid region accompanying alkaline regions at the both sides, respectively.[12] The passive flux, the active flux and the total flux as well as the contour lines of H^+ concentration are shown. The numerical result of the total flux has a characteristic M-shaped pattern, which agrees with the experimental observation.[14] This type of flux pattern indicates a circulation of H^+ flux from the acid region to the alkaline region. Figure 8 may confirm this expectation, where the streamlines are drawn so as to cross perpendicularly to the contour lines in a band pattern with three acid regions.

Figure 9 shows an example of formation process of bands arising from the homogeneous state when the light intensity is abruptly increased.[12] A remarkable feature is that the M-shaped pattern appears
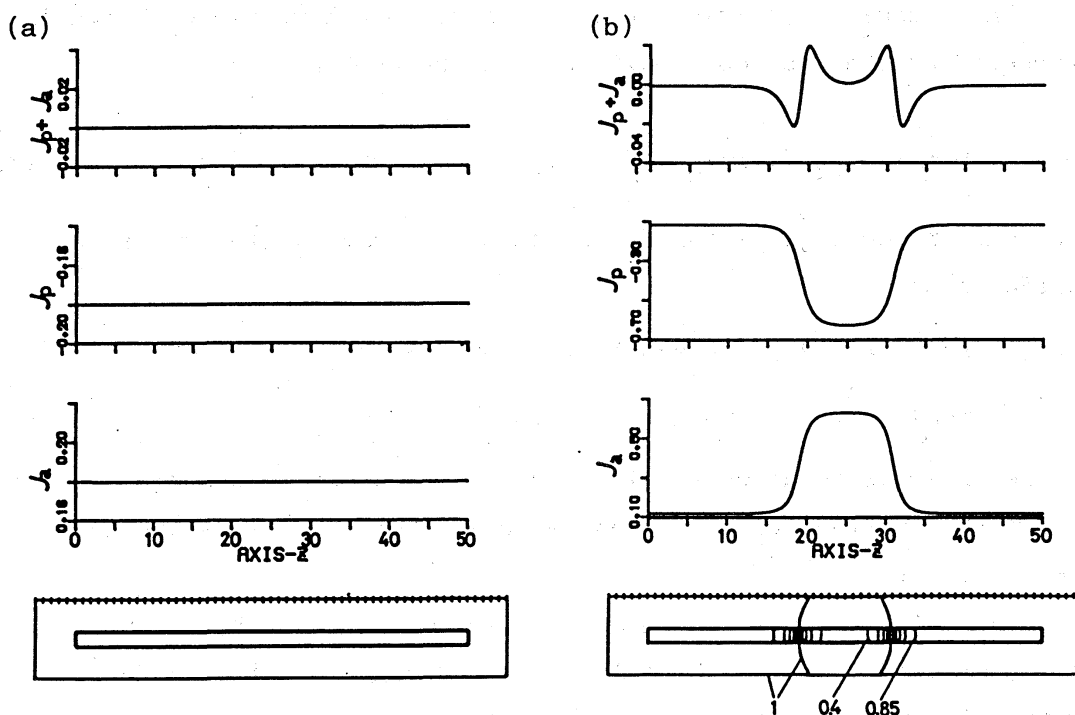
(a)

(b)

Fig.7 Flux patterns of the homogeneous and band states. Numerical parameters are p=1, D=3, α =0.75, γ =0.153, a=1, R=0.85 and L=50. (a) I=0.18; (b) I=0.24. The step size of contour lines is 0.05.
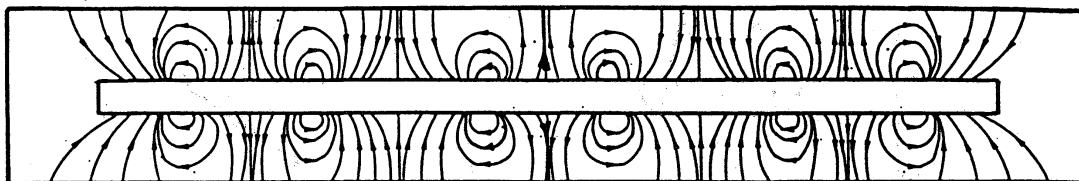
Fig.8 Flow pattern of protons. Since the external boundary condi-
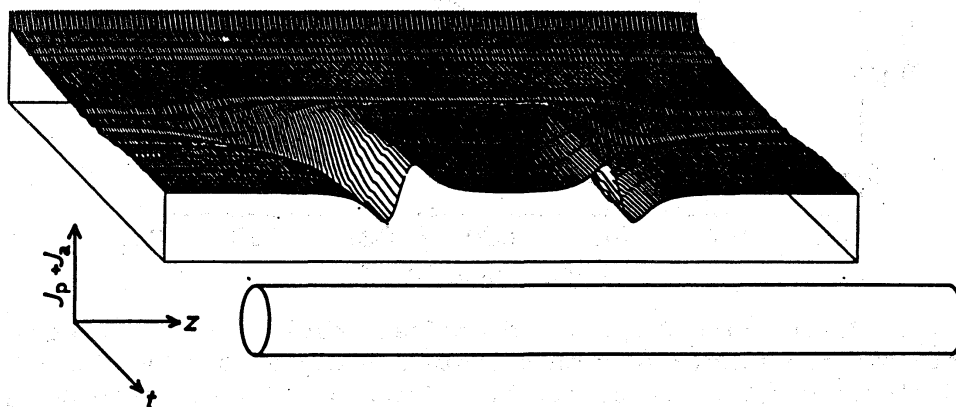tion is taken as a reservoir of n=1.0, the H+ flux occurs there.

Fig.9 Dynamics of the band formation from the homogeneous state.
The light intensity is increased abruptly from I=0.18 to I=0.28.

dramatically after the transitory increase in flux along the overall
cell length. Similar changes are also observed in experiments.[15,16]

Figure 10 shows the bifurcation diagram in terms of the band width
ℓ for the external variable I.[12] The band pattern with the finite
band width appears suddenly at a critical value, I_c, but disappears to
recover the homogeneous state at the different value of I for decreas-
ing I. These facts for the existence of the critical light intensity
and the appearance of hysteresis are reproducing well the experimental
observation.[17] The bifurcation phenomenon obtained numerically can
be explained from a linear stability analysis and a local potential
proposed by Prigogine to give some intuitive understanding for the
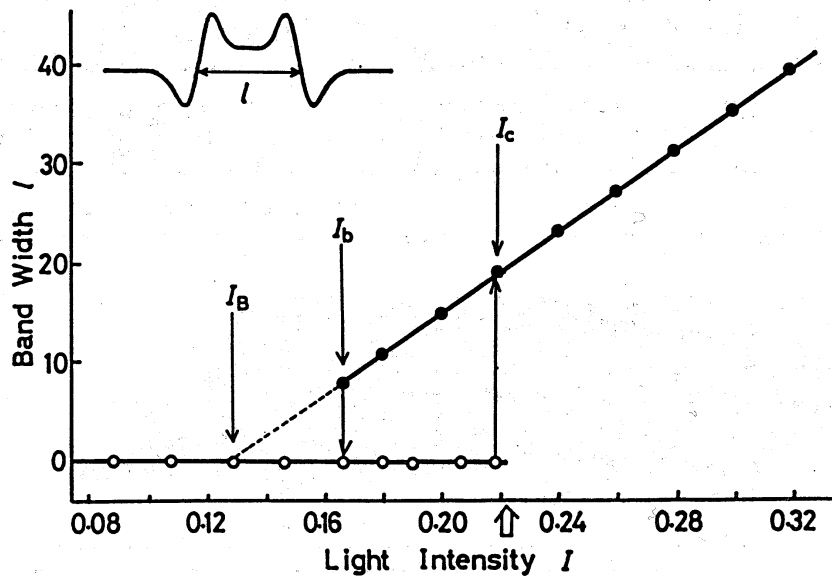occurrence of self-organized state.[7]

Fig.10 Bifurcation diagram. Numerical results of the homogeneous state and the single-acid band state are designated by open circles and closed circles, respectively. Thick solid lines show analytical result. The bifurcation point predicted by eq.(13) is denoted by a large arrow on the I-axis.

3.3 Analytical results

A stationary homogeneous solution is given by

$$n^0 = \begin{cases} N_e = 1 & \text{at } r > R , \\ N_i = 1 - a\,I/p & \text{at } r < R , \end{cases}$$ (10)

$$h^0 = a\,I/p + \gamma \ln[\alpha/aI - 1] .$$ (11)

The stationary H^+-concentration difference Δn^0 becomes

$$\Delta n^0 = N_e - N_i = a\,I/p .$$ (12)

Applying the linear stability analysis to the present model system, we can straightforwards get the expression for the critical light intensity:[12)]

$$I_c = \left\{ \alpha - \sqrt{\alpha^2 - 4\gamma\alpha[p + (\frac{k\pi}{L})^2\frac{DR}{2}]} \right\}/2a ,$$ (13)

with k denoting the integer. If we substitute the parameter values shown in Fig.7, $I_c = 0.221$ can be obtained for the one-band pattern.

This value shows a good agreement with the numerical value 0.218. Thus, the linear stability analysis predicts the stable homogeneous solution below I_c and the unstable homogeneous solution above I_c giving rise to the appearance of band-type pattern.

In the present system, we can introduce the generalized fluxes J and the generalized forces X by

$$J_1 = J_p \ , \ X_1 = -\Delta n/\Delta r$$
$$J_2 = J_a \ , \ X_2 = (h-\Delta n)/\Delta r$$
at the membrane,

$$J_3 = -D\nabla n \ , \ X_3 = -\nabla n \qquad \text{in the cell exterior and interior,} \qquad (14)$$

where Δr is the membrane thickness. The local potential Φ can be obtained by using its definition as follows:[7,12]

$$\Phi = 2\pi R \int_0^L \phi \ dz \ , \qquad (15)$$

with ϕ denoting a local potential per unit length:

$$\phi = \frac{p}{2}(\Delta n)^2 + \alpha(h-\Delta n) - \gamma\alpha \ln\left[1+\exp\left(\frac{h-\Delta n}{\gamma}\right)\right]$$
$$+ \frac{D}{2}\alpha_k^2 R K_1 I_1 (\Delta n - \Delta n^0)^2 - aIh \ . \qquad (16)$$

In this expression, α_k is defined by

$$\alpha_k = k\pi/L \qquad \text{for } k=1, 2, \cdots \qquad (17)$$

and K_ν and I_ν are the modified Bessel functions of ν-th order dependent on $\alpha_k R$. It is to be noted that Δn is a function of the spatial coordinate z alone and h is independent of z.

The stationary point is given by eq.(15) with eq.(16) as

$$\frac{\partial\phi}{\partial(\Delta n)} = p\Delta n + D\alpha_k^2 R K_1 I_1 (\Delta n - \Delta n^0) - \frac{\alpha}{1+\exp[(h-\Delta n)/\gamma]} = 0, \qquad (18a)$$

$$\frac{\partial\Phi}{\partial h} \propto \frac{1}{L}\int_0^L \frac{\alpha}{1+\exp[(h-\Delta n)/\gamma]} \ dz - aI = 0 \ . \qquad (18b)$$

/ /

In the homogeneous state of $\Delta n = \Delta n^0 = $ const. and $h = h^0 = $ const, the above equations are reduced to the stationary solution (10) ~ (12).

From a comparison with the linear stability analysis, we can easily show that the potential ϕ is minimum at the stable homogeneous state but is maximum at the unstable state. Note that $\phi = \Phi/2\pi RL$ is equivalent to Φ itself in the homogeneous state. Figure 11 shows a schematic illustration of ϕ for the homogeneous state on the I-Δn plane.[12] The stable homogeneous solution exists until the minimum point changes its position to the maximum with increasing I, so that the stability changes at $I=I_c$. This situation is analogous to a first-order phase transition in equilibrium systems.

Let us next investigate the self-organized state realizing as a result of the instability of homogeneous state. For this purpose, we had better approximate $\Delta n(z)$ in the single-acid band state as (see Fig.12)

$$\Delta n = \begin{cases} \Delta n_h & \text{for } (L-\ell)/2 \leq z \leq (L+\ell)/2 \quad , \\ \\ \Delta n_\ell & \text{otherwise,} \end{cases} \qquad (19)$$
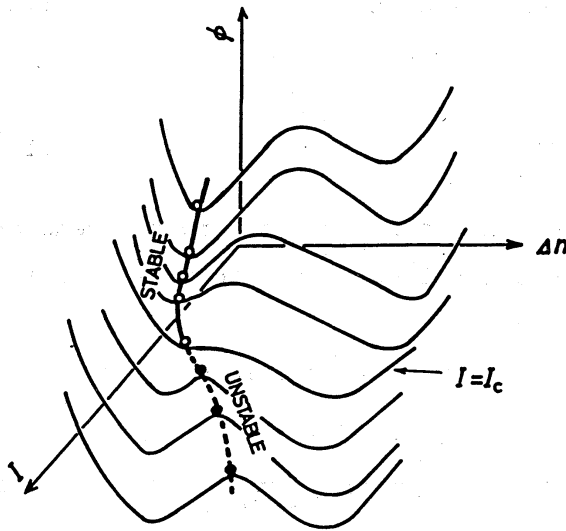

Fig.11 Schematic illustration of the stability of homogeneous state in terms of the local potential per unit length.
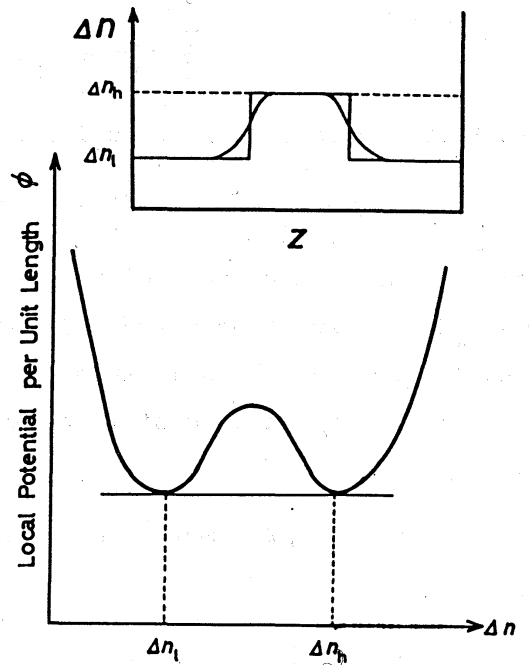

Fig.12 The local potential per unit length for the band-pattern state.

where ℓ is the band width. Two quantities Δn_h and Δn_ℓ are given respectively by $\Delta n = \Delta n_h$ and Δn_ℓ in eq.(18a). When eq.(19) is substituted into eq.(18b), we get

$$(\Delta n_h - \Delta n_\ell)\frac{\ell}{L} + \Delta n_\ell = \frac{Ia}{p} . \qquad (20)$$

This equation gives ℓ as a function of I, and is shown by a solid line in Fig.10. A good agreement with the numerical results can be seen.

The local potential Φ can be written from eqs.(15), (16) and (19) by

$$\Phi = 2\pi R \left[\phi(\Delta n_\ell, h^*)(L-\ell) + \phi(\Delta n_h, h^*)\ell \right] \qquad (21)$$

with h^* denoting h in the band state. Minimizing Φ with respect to ℓ gives

$$\phi(\Delta n_\ell, h^*) = \phi(\Delta n_h, h^*) . \qquad (22)$$

This result is quite impressive: the local potential per unit length in the lower Δn region is equal to that in the higher Δn region. The alkaline band and the acid band keep their balance in the sense of the equal ϕ. The situation is illustrated in Fig.12. The local potential per unit length can, therefore, be regarded as a chemical potential in equilibrium systems.

Dynamics from the homogeneous state to the band state can be described by the use of the kinetic equation dominated by the local potential:[12)]

$$R K_1 I_1 \frac{\partial(\Delta n)}{\partial t} = - \frac{\partial \phi}{\partial(\Delta n)} , \qquad (23)$$

If we limit our description to the neighborhood of the stationary homogeneous state, Δn can be written as

$$\Delta n = \Delta n^0 + \delta \Delta n \qquad (24)$$

with $\delta \Delta n$ implying a small quantity.

By taking account of the condition on h given by eq.(18b), we get the final equation for $\delta \Delta n$:[12)]

$$\left(\frac{\partial}{\partial t} - D\frac{\partial^2}{\partial z^2}\right)\delta\Delta n = \frac{1}{RK_1 I_1}\left[-p + \frac{\alpha(\alpha/Ia-1)}{\gamma(\alpha/Ia)^2}\right]\delta\Delta n$$

$$+ \frac{\alpha(\alpha/Ia-1)(\alpha/Ia-2)}{2\gamma^2 RK_1 I_1(\alpha/Ia)^3}\left[(\delta\Delta n)^2 - <(\delta\Delta n)^2>\right], \qquad (25)$$

with

$$<(\delta\Delta n)^2> = \frac{1}{L}\int_0^L (\delta\Delta n)^2\, dz\ . \qquad (26)$$

For the unstable homogeneous state the coefficient of the first term takes a positive value. The coefficient of the second term is also positive. This term acts to increase $\delta\Delta n$ in the region where $(\delta\Delta n)^2$ once overcomes the average value $<(\delta\Delta n)^2>$, but to decrease $\delta\Delta n$ where $(\delta\Delta n)^2$ is below $<(\delta\Delta n)^2>$. In other words, this constitutes a positive-feedback origin in the formation of a spatial pattern composed of two types of regions with a higher and a lower magnitude of Δn. Figure 13 illustrates a behavior of the system in terms of ϕ on the h-Δn plane beyond the bifurcation point.[12]
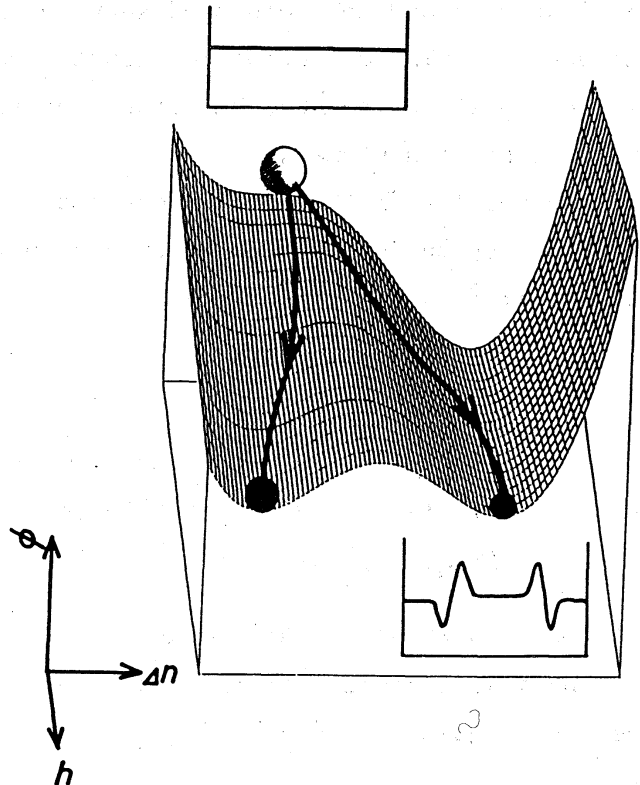

Fig.13 Dynamic change from the homogeneous state to the band-pattern state.

The present model system can explain well many observed data such as the occurrence of bands beyond the critical light intensity, the hysteresis, the M-shaped flux pattern, dynamics of band formation and so on. In this case the local potential per unit length ϕ helps us to understand the properties of theoretical model system.

Last, we must mention some points. The first is the effect of Ca^{2+} ions on the band formation. The $CaCO_3$ deposition facilitates the desired positioning of the acid and alkaline zones.[18] To explain this experimental fact, electrochemical studies[19,20] of the interaction between Ca^{2+} and the membrane structure may be necessary. The second point is concerned with the hysteresis. The present theoretical analysis is inadequate to explaining it, because the description is limited to the bifurcation point. This type of hysteresis may be related to an inverted or subcritical bifurcation.[21] An improvement of theoretical analysis is one of the future works.

4. Discussion

In the theoretical model, the angular dependence was not taken into account. It arises from a theoretical conclusion that a symmetry breaking along a longitudinal axis appears before the one along a circumferential direction.[13] This conclusion holds generally in a unit-cell or many-cell system of a cylindrical shape, accompanied by the surrounding electric current. In fact, the green alga *Acetabularia* exhibits a band-type pattern of chloroplasts.[13,22]

In bean roots self-sustained oscillations of surface electric potential were observed near the root tip for many cases. As shown in Fig.14, the periods of oscillations were composed of the integer ratio of 6, 12, 18 min with the amplitudes 1.5, 3.0 and 4.5 mV, respectively. They changed mutually with time. This curious occurrence of oscillations may reflect some relationship between the cellular process and the membrane transport. Self-sustained oscillations of electric potential have been often observed in the case of growth and regeneration.[1-3] These kinds of oscillations have been also found in much simpler systems of model membrane constructed from lipids and/or proteins.[23-25] In these systems an importance of

electrochemical interaction between cations and the membrane is pointed out. Oscillations in the growth could, therefore, be understood more definitely based on electrochemical studies taking account of non-equilibrium situations.
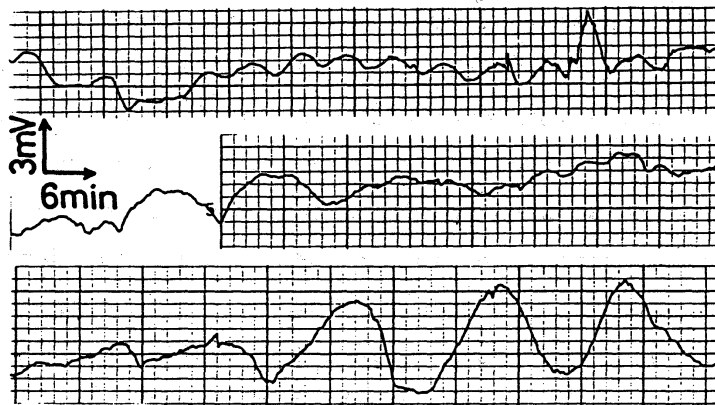

Fig.14 Self-sustained oscillations of the electric potential near the root tip.

References

1) L.F. Jaffe: Membrane Transduction Mechanism, eds. R.A. Cone and J. E. Dowling (Raven Press, New York, 1979) p.199.

2) B. Novak: Adv. Chem. Phys. 29 (1975) 281.

3) B.I.H. Scott: Ann. N. Y. Acad. Sci. 98 (1962) 890.

4) N.A. Walker and F.A. Smith: J. Exp. Bot. 28 (1977) 1190.

5) K. Toko and K. Yamafuji: Biophysics (Kyoto) 23 (1983) 76.

6) K. Toko and K. Yamafuji: J. Phys. Soc. Jpn. 51 (1982) 3049.

7) P. Gransdorff and I. Prigogine: Thermodynamic Theory of Structure, Stability and Fluctuations (Wiley-Interscience, London, 1971).

8) D. Feinn, P. Ortoleva, W. Scalt, S. Schmidt and M. Woltt: J. Chem. Phys. 69 (1978) 27.

9) S. Iiyama, K. Toko and K. Yamafuji: submitted to Biophys. Chem.

10) D.L. Rayle and R.E. Cleland: Plant Physiol. 46 (1970) 250.

11) D.J. Spear, J.K. Barr and C.E. Barr: J. Gen. Physiol. 54 (1969) 397.

12) K. Toko, H. Chosa, K. Ryu and K. Yamafuji: submitted to J. Theor. Biol.

13) K. Toko, S. Iiyama and K. Yamafuji: submitted to J. Phys. Soc. Jpn.

14) W.J. Lucas and R. Nuccitelli: Planta 150 (1980) 120.

15) J.M. Ferrier and W.J. Lucas: J. Exp. Bot. 30 (1979) 705.

16) K. Ogata: Plant Cell Physiol. 24 (1983) 695.

17) W.J. Lucas: J. Exp. Bot. 26 (1975) 347.

18) F.A. Smith and N.A. Walker: J. Memb. Biol. 73 (1983) 193.

19) K. Toko and K. Yamafuji: Biophys. Chem. 14 (1981) 11.

20) K. Toko and K. Yamafuji: J. Theor. Biol. 99 (1982) 461.

21) K. Yamafuji, K. Toko and K. Urahama: J. Phys. Soc. Jpn. 50 (1981) 3819.

21) M. Paques, C. Sironval and S. Bonotto: Developmental Biology of *Acetabularia*, eds. S. Bonotto, V. Kefeli and S. Puiseux-Dao (Elsevier/North-Holland, Amsterdam, 1979) p.155.

23) Y. Kobatake: Adv. Chem. Phys. 29 (1975) 319.

24) K. Toko, K. Ryu, S. Ezaki and K. Yamafuji: J. Phys. Soc. Jpn. 51 (1982) 3398.

25) K. Toko, M. Tsukiji, S. Ezaki and K. Yamafuji: Biophys. Chem. 20 (1984) in press.